https://dx.doi.org/10.22161/ijaers.5.5.33 ISSN: 2349-6495(P) | 2456-1908(O)

Resistance Spot Welding of Dissimilar Steels: Temperature Curves

Diego Fonseca Silva[1], Pedro Paiva Brito[2], Pedro Américo Almeida Magalhães Júnior[3], Thaís Roberta Campos[4]

[1]Department of Engineering Mechanincal, Pontifícia Universidade Católica de Minas Gerais, Brasil
Email: diegofonsecasilva@yahoo.com.br
[2]Department of Engineering Mechanincal, Pontifícia Universidade Católica de Minas Gerais, Brasil
Email: ppbrito@gmail.com
[3]Department of Engineering Mechanincal, Pontifícia Universidade Católica de Minas Gerais, Brasil
Email: paamjr@gmail.com
[4]Department of Engineering Mechanincal, Pontifícia Universidade Católica de Minas Gerais, Brasil
Email: trcampos@sga.pucminas.br

***Abstract*— *Resistance spot welding was used to joint AISI 316L austenitic stainless steel and AISI 1020 low carbon steel. During the welding process, temperature measurements were taken to obtain the temperature curves. Because of the different chemical compositions of the carbon steel and stainless steels, their thermal conductivity values are also different. Electrical resistivity is also an important parameter when carbon steel is spot welded to stainless steel. Differences in the thermal conductivity and in the electrical resistivity of metals lead to an asymmetrical weld nugget in the dissimilar joints. Dissimilar resistance spot welding can be more complex than similar welding due to different thermal cycle experienced with each metal.*

***Keywords*— Carbon steel, spot welding, stainless steel, temperature curves, thermal conductivity.**

I. INTRODUCTION

The spot welding process joints two or more metal sheets together through fusion at certain point. It is a simple process that uses two copper electrodes to press the work sheets together and high current to pass through it. The growth of weld nugget is, therefore, determined by its controlling parameter such as current, weld time, electrode tips, and force. The Fig. 1 shows the schematic of the spot weld.

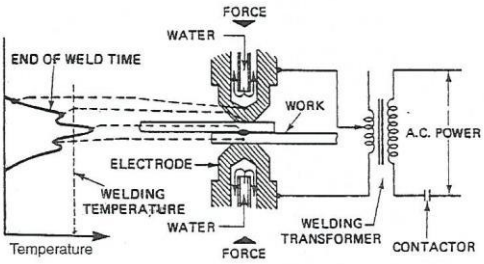

Fig. 1: Resistance spot welding

The generation of heat is due to resistance to current flow, this phenomenon is known as joule effect. The total thermal energy generated during the welding process can be calculated by Joule's law:

$$Q = \frac{1}{J}\int_0^t I^2 R_T \, dt \quad (1)$$

Where:
J – 4,185 [J];
I – Welding Current [A];
R_T – Electrical Resistance [Ω];
dt – time interval [s].

The schematic of the electrical resistances of the spot welding process is shown in Fig. 2.

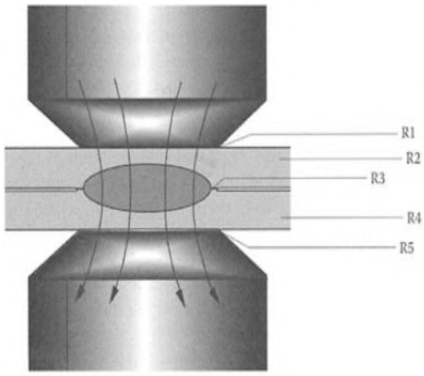

Fig. 2: Electrical Resistances

In dissimilar joints, one of the important features of the weld nugget is its asymmetrical shape such that fusion zone size and penetration depth of stainless steel side are larger than those of carbon steel side. Electrical resistance and thermal conductance control heat generation and heat

https://dx.doi.org/10.22161/ijaers.5.5.33 **ISSN: 2349-6495(P) | 2456-1908(O)**

dissipation which in turn, effect weld nugget formation and its growth.

Differences in the thermal conductivity and electrical resistivity of two steel sheets lead to an asymmetrical weld nugget in dissimilar metal joints. Lower electrical resistance of carbon steel, and its higher thermal conductivity compared to stainless steel leads to smaller fusion zone in the former.

The joint region consists of three distinct structural zones: fusion zone (FZ) or weld nugget, heat affected zone (HAZ) and base metal (BM).

The Fig. 3 shows a typical geometric morphology of resistance spot weld.

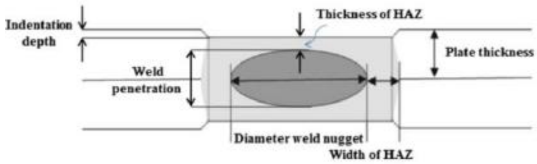

Fig. 3: Geometric morphology

II. EXPERIMENTAL PROCEDURE

The materials used in the present work were AISI 1020 carbon steel and AISI 316L austenitic stainless steel in the form of 1x 25 x 100 mm sheets. The nominal chemical composition of both steels is presented in TABLE 1.

Table 1 – The Chemical Composition of materials, Wt.%

Steel:	C	Mn	Cr	Ni	Si
AISI 1020	0,18-0,23	0,30-0,60	-	-	-
AISI 316L	0,03	2,00	18,00	14,00	0,75

During welding, the length of the overlap between both sheets was 25 mm, as depicted in Fig 4.

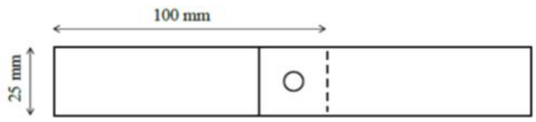

Fig. 4: Geometry of the overlap joints

The welding parameters were fixed, welding current 13kA, welding time 1 s and constant pressure. Fig. 5 shows spot welding machine used.

Fig. 5: Spot Welding Machine used in this investigation

In the temperature measurement procedure, three thermocouples type K were used. The first thermocouple was placed in heat affected zone (HAZ), the second thermocouple 1cm distant from the (HAZ), the third thermocouple 2 cm distant from the (HAZ). Fig. 6 shows positioning of the thermocouples in the sheets.

Fig. 6: Thermocouples type k

III. RESULTS AND DISCUSSION

The Fig. 7 and Fig. 8 shown the values obtained in the measurements of temperature in the sheets of stainless steel and carbon steel, respectively.

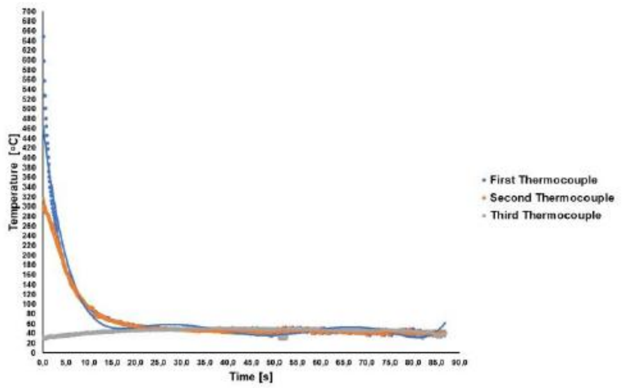

Fig. 7: Temperature curves – sheet 316 L

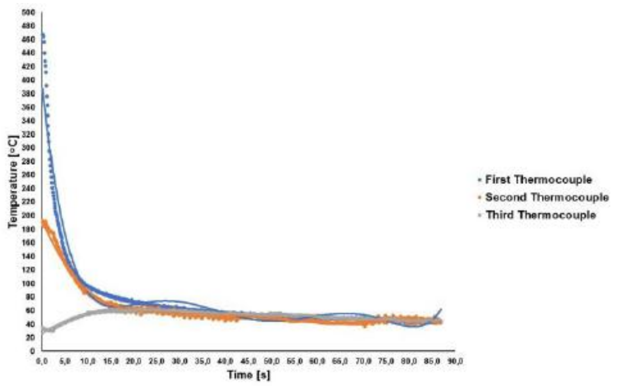

Fig. 8: Temperature curves – sheet 1020

One of the ways to evaluate the quality of fit of the model is through the coefficient of determination R^2. Basically, this coefficient indicates how much the model was able to

https://dx.doi.org/10.22161/ijaers.5.5.33 ISSN: 2349-6495(P) | 2456-1908(O)

explain the data collected. The coefficient of determination R^2 is given by the expression:

$$R^2 = \frac{\left(\sum_{i=1}^{n}(x_i - \bar{x})Y_i\right)^2}{\sum_{i=1}^{n}(x_i - \bar{x})^2 \sum_{i=1}^{n}(Y_i - \bar{Y})^2} \qquad (2)$$

Where,

$$0 \leq R^2 \leq 1 \qquad (3)$$

The Fig. 9 and Fig. 10 shown the coefficient of determination R^2 values obtained in the curves of temperature. The 6th degree polynomial was used.

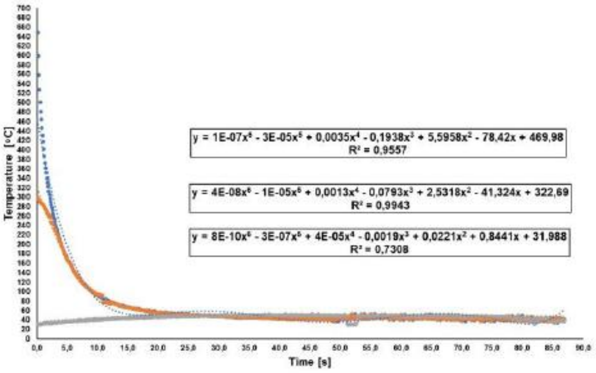

Fig. 9: Coefficient of determination R^2 – sheet 316 L

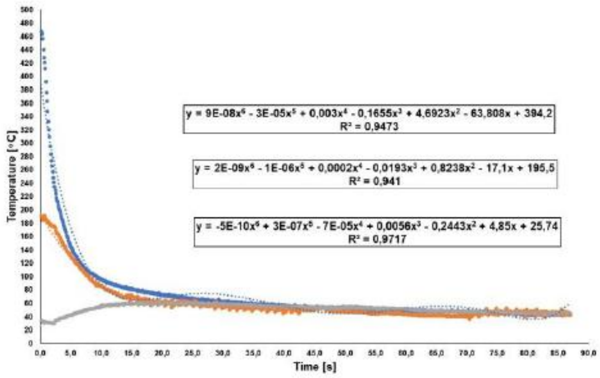

Fig. 10: Coefficient of determination R^2 – sheet 1020

The TABLE 2 and TABLE 3 show values of the coefficient of determination R^2 in relation to the position of the thermocouple in the stainless steel and carbon steel sheets, respectively.

Table 2 – Values of Coefficient of determination R^2 (sheet 316L)

Thermocouple:	Position	R^2
First	HAZ	0,9557
Second	1 cm of HAZ	0,9943
Third	2 cm of HAZ	0,7308

Table 3 – Values of Coefficient of determination R^2 (sheet 1020)

Thermocouple	Position	R^2
First	HAZ	0,9473
Second	1 cm of HAZ	0,941
Third	2 cm of HAZ	0,9717

IV. CONCLUSION

In the dissimilar spot welding of AISI 1020 carbon steel and AISI 316 L stainless steel, the temperature curves obtained show that the materials undergo different thermal cycles, this is expected because the steels have different chemical compositions and thermal properties. That is, the results are in agreement with the theory.

The coefficients of determination R^2 obtained in the 1020 carbon steel sheet and the 316L stainless steel sheet have values very close to 1, that is, the fit of the model was good. Except, the third thermocouple of the stainless steel sheet (R^2 = 0,7308).

ACKNOWLEDGEMENTS

The authors gratefully acknowledge FAPEMIG and PUC-MG for assistance in publication of this work.

REFERENCES

[1] ALENIUS, M. et al. Exploring the mechanical properties of spot welded dissimilar joints for stainless and galvanized steels. **Welding research**, Finland, p. 305-313, 2006.

[2] MARASHI, P. et al. Microstructure and failure behavior of dissimilar resistance spot welds between low carbon galvanized and austenitic stainless steels. **Materials science and engineering**, Tehran, p.175-180, 2008.

[3] KOLARIK, Ladislav et al. Resistance spot welding of dissimilar steels. **Acta polytechnica**, Praha, p. 43-47, 2012.

[4] POURANVARI, M. et al. Similar and dissimilar RSW of low carbon and austenitic stainless steels: effect of weld microstructure and hardness profile on failure mode. **Materials science and technology**, Dezful, p. 1411-1416, 2009.

[5] ABADI, Mehdi Mansouri Hasan et al. Correlation between macro/micro structure and mechanical properties of dissimilar resistance spot welds of AISI 304 austenitic stainless steel and AISI 1008 low carbon steel. **Association of metallurgical engineers of Serbia – AMES**, Iran, p. 133-146, 2010.

[6] ARAVINTHAN, A. et al. Analysis of spot weld growth on mild and stainless steel. **Supplement to the welding journal**, Malaysia, p.143-147, 2011.

[7] FARIA, André Luiz Oliveira de et al. Dissimilar resistance spot welding of AISI 1010 carbon steel and AISI 304 austenitic stainless steel. In: 8th BRAZILIAN CONGRESS OF MANUFACTURING ENGINEERING, 2015, Bahia.

[8] POURANVARI, M. et al. Critical review of automotive steels spot welding: process, structure and properties. **Science and technology of welding and joining**, Tehran, p. 361-403, 2013.

[9] KIANERSI, Danial et al. Resistance spot welding joints of AISI 316L austenitic stainless steel sheets: phase transformation, mechanical properties and microstructure characterization. **Materials and design**, Tehran, p. 251-263, 2014.

[10] HASANBASOGLU, Ahmet et al. Resistance spot weldability of dissimilar materials (AISI 316L – DIN EN 10130-99 steels). **Materials and design**, Karabuk, p. 1794-1800, 2007.

[11] KOCABEKIR, Bayram et al. An effect of heat input, weld atmosphere and weld cooling conditions on the resistance spot weldability of 316L austenitic stainless steel. **Journal of materials processing technology**, Karabuk, p. 327-335, 2008.

[12] MARASHI, P. et al. Relationship between failure behavior and weld fusion zone attributes of austenitic stainless steel resistance spot welds. **Materials science and technology**, Tehran, p. 1506-1512, 2008.

[13] POURANVARI, M. et al. Failure mode of dissimilar resistance spot welds between austenitic stainless and low carbon steels. **Metal 2008**, Tehran, p. 1-6, 2008.

[14] MOSHAYEDI, Hessamoddin et al. Resistance spot welding and the effects of welding time and current on residual stresses. **Journal of materials processing technology**, Tehran, p. 2545-2552, 2014.

[15] POURANVARI, M. et al. Failure mode transition in AHSS resistance spot welds. Part I. Controlling factors. **Materials science and engineering**, Tehran, p. 8337-8343, 2011.

[16] KIANERSI, Danial et al. Effect of welding current and time on the microstructure, mechanical characterizations, and fracture studies of resistance spot welding joints of 316L austenitic stainless steel. **Metallurgical and materials transactions**, Tehran, 2014.

[17] POURANVARI, M. et al. Effect of weld nugget size on overload failure mode of resistance spot welds. **Science and technology of welding and joining**, Tehran, p. 217-225, 2007.

[18] ASLANLAR, S. et al. Welding time effect on mechanical properties of automotive sheets in electrical resistance spot welding. **Materials and design**, Sakarya, p. 1427-1431, 2008.

[19] FUKUMOTO, Shinji et al. Small-scale resistance spot welding of austenitic stainless steels. **Materials science and engineering**, Hyogo, p. 243-249, 2008.

[20] CHARDE, Nachimani et al. Materials characterizations of mild steels, stainless steels, and both steel mixed joints under resistance spot welding. **Int j adv manuf technol**, Malaysia, p. 373-384, 2014.

[21] ALENIUS, M. T. et al. Mechanical and corrosion properties of spot-welded high-strength austenitic stainless steel EN 1.4318. **Materials and corrosion**, Finland, p. 296-302, 2008.